ANALYTICAL EXPRESSION FOR FRESNEL VOLUMES AND INTERFACE FRESNEL ZONES OF SEISMIC BODY WAVES. PART 1: DIRECT AND UNCONVERTED REFLECTED WAVES

MICHAL KVASNIČKA, VLASTISLAV ČERVENÝ

Department of Geophysics, Charles University, Prague[*]

Summary: *Fresnel volumes, plane-sectional Fresnel zones and interface Fresnel zones of direct and unconverted reflected waves are studied. Exact analytical expressions for various parameters of Fresnel volumes and Fresnel zones are derived and discussed. Among others, these expressions are related to semi-axes of Fresnel zones, to overshooting and penetration distances, and to the off-ray shifts of Fresnel zones.*

Keywords: Fresnel volumes, interface Fresnel zones, seismic body waves, seismic ray methods, first arrival travel times

1. INTRODUCTION

A Fresnel volume represents the spatial vicinity of the mathematical ray trajectory which actually influences the wave field at the receiver. The width of the Fresnel volume is frequency-dependent: it is narrow for high frequencies and broader for small frequencies. In a homogeneous medium, it is approximately proportional to $f^{-1/2}$, where f denotes the frequency. Only in the infinite-frequency limit, the Fresnel volumes reduce to the volumeless mathematical rays. Fresnel volumes are known under many names, such as physical rays, 3-D Fresnel zones, regions responsible for diffraction, fat rays, etc.

The section of the Fresnel volume by a plane perpendicular to the relevant ray is called *Fresnel zone*. In a similar way, we shall call the section of the Fresnel volume by an arbitrarily oriented plane the *plane-sectional Fresnel zone*, and the section of the Fresnel volume by an interface the *interface Fresnel zone*.

The commonly used definition of Fresnel volumes is based on the travel-time concepts and was proposed by *Kravtsov and Orlov (1979, 1980)*. Let us consider a monochromatic harmonic wave field with period T and frequency $f = 1/T$, and assume the point source situated at S and receiver at R. The Fresnel volume corresponding to the source at S and receiver at R is formed by points F which satisfy the following condition:

$$\left|\tau(F,S)+\tau(F,R)-\tau(S,R)\right| \le \frac{1}{2}T \quad . \tag{1}$$

Here $\tau(F,S)$ represents the travel time from F to S, $\tau(F,R)$ the travel time from F to R, and $\tau(S,R)$ the travel time from S to R. The boundary of the Fresnel volume is than given by the following equation:

[*] Address: Ke Karlovu 3, 121 16 Praha 2, Czech Republic
(Fax: +422-21911292, E-mail: qasnicka@seis.karlov.mff.cuni.cz)

Studia geoph. et geod. 40 (1996), 136-155

$$\left|\tau(F,S)+\tau(F,R)-\tau(S,R)\right| = \frac{1}{2}T \quad . \tag{2}$$

Point F is usually called the *virtual point*. The physical meaning of (1) and (2) is quite clear. For virtual points such that the time difference between $\tau(F,S) + \tau(F,R)$ and $\tau(S,R)$ is less than one half of the period, the interference is constructive.

Seismic wave fields, however, are not monochromatic, but transient. Seismic signals are usually represented by short wavelets, the Fourier spectrum of which contains many frequencies. For narrow-band seismic signals, the monochromatic Fresnel volumes constructed for the prevailing frequency of the signal, may represent a good approximation of the Fresnel volume relevant to the signal. Otherwise, it would be necessary to consider Fresnel volumes for several frequencies. See also *Knapp (1991)*.

Recently, Fresnel volumes and related Fresnel zones have found many applications in seismology and in seismic exploration. Traditionally, they have played an important role in the investigations of the resolution of seismic methods (*Sheriff, 1977, 1980, 1985, 1989; Sheriff and Geldart, 1982; Kleyn, 1983; Lindsey, 1989; Almeida, 1991; etc.*). Fresnel volumes have also been used to study the accuracy of the ray method (*Kravtsov and Orlov, 1979, 1980, 1990; Ben-Menahem and Beydoun, 1985; Beydoun and Ben-Menahem, 1985; Kravtsov, 1988*). They have been applied in tomographic studies and in other methods of inversion of seismic data (*Yomogida, 1992*). *Klimeš (1994)* also proposed a method in which Fresnel volumes are applied to increase the accuracy of network ray tracing. The authors expect that Fresnel volumes will find soon many other applications both in forward and in inverse seismic methods.

Two methods have been proposed to compute Fresnel volumes in complex 2-D and 3-D structures. The *first method*, called *Fresnel volume ray tracing*, proposed by *Červený and Soares (1992)*, is based on the approaches of the paraxial ray approximation. It consists in standard numerical ray tracing, supplemented by dynamic ray tracing. Dynamic ray tracing is used to compute the complete ray propagator matrix, which is needed to evaluate the Fresnel volumes. Since dynamic ray tracing and the computation of the ray propagator matrix have been recently used as the standard procedure in most ray tracing packages, Fresnel volume ray tracing is simple to program and is numerically very efficient. The paraxial ray methods, however, are only approximate and are applicable only to zero-order ray theory waves (direct, reflected, transmitted, multiply reflected, etc.) but not to higher-order waves (head waves) and to diffracted waves. The half-width of the Fresnel volume and the Fresnel zones are usually of the order of $f^{-1/2}$, where f is the frequency. Effects such as overshooting, penetration, off-ray shifts, etc., which are of the order of f^{-1}, cannot be obtained by Fresnel volume ray tracing. See also *Gelchinsky (1985)*.

The *second method*, proposed recently by *Kvasnička and Červený (1994)* is based on network ray tracing. For details on network ray tracing refer to *Moser (1991,1992)* and *Klimeš and Kvasnička (1994)*. The method is applicable to first arriving waves only, but may also be applied to waves which do not belong to the category of zero-order ray theory waves (head waves, diffracted waves in shadow zones, etc.). By a simple modification of the network ray tracing procedure, the method may be applied even to the computation of Fresnel volumes of reflected waves, although these waves do not appear in first arrivals. This method is considerably more accurate than the Fresnel volume ray tracing, and also yields effects of the order of f^{-1} (which are not obtained by Fresnel volume ray tracing).

The above two methods cannot be applied to obtain exact analytical results. The analytical results are, however, important in various applications. Moreover, the analytical results offer us a deeper insight into the properties of Fresnel volumes and Fresnel zones.

This is the main reason why this paper presents the exact analytical computations relevant to Fresnel volumes and Fresnel zones. These analytical computations, however, refer only to simple structures (homogeneous media, a plane interface between two homogeneous halfspaces, etc.). Most

of the derived expressions are exact. Even in simple structures, however, exact analytical solutions are not always available. If this is so, we at least try to give the equation from which the exact results may be obtained numerically. Anyway, we always give some approximate analytical solutions. However, effects of the order of f^{-1} are also obtained, and these cannot be calculated by paraxial ray methods (Fresnel volume ray tracing).

This paper is devoted to direct waves and to unconverted reflected waves. These two types of waves play the most important roles in seismic applications. Part 2 of this paper, see *Kvasnička and Červený (1996)*, will be devoted to head waves, and to transmitted and converted waves.

2. FRESNEL VOLUMES AND FRESNEL ZONES IN HOMOGENEOUS MEDIUM

Let us consider a monochromatic direct wave, frequency f, propagating in a homogeneous medium from a point source situated at S to a receiver point at R. The distance between S and R is l and the propagation velocity v.

2.1 Fresnel volume of a direct wave as an ellipsoid of revolution

It is not difficult to prove that the Fresnel volume of a direct wave in a homogeneous medium is an ellipsoid of revolution, its rotational axis passing through S and R. To prove this, we introduce a local Cartesian coordinate system x,y,z with its origin at point O, situated in the middle between S and R, the x-axis coinciding with the straight line $\overline{SR}$. The x-coordinates of points S, O, R are $-\frac{1}{2}\ell$, 0, $\frac{1}{2}\ell$, respectively. Equation (2) for the boundary of the Fresnel volume can then be expressed in the following form:

$$\left[\left(x-\frac{\ell}{2}\right)^2+r^2\right]^{1/2}+\left[\left(x+\frac{\ell}{2}\right)^2+r^2\right]^{1/2}-\ell=\frac{1}{2}\lambda \quad ,$$

where $r^2=y^2+z^2$, and λ is the wavelength, $\lambda=vT=v/f$. After some simple algebra, this equation yields the equation of the ellipsoid of revolution,

$$\frac{x^2}{a^2}+\frac{y^2+z^2}{b^2}=1 \quad , \tag{3}$$

where a, b are the semi-axes of the ellipsoid:

$$a=\frac{1}{2}\ell\left(1+\frac{1}{2}\frac{\lambda}{2}\right) \quad , \qquad b=\frac{1}{2}\sqrt{\lambda\ell}\left(1+\frac{1}{4}\frac{\lambda}{\ell}\right)^{1/2} \quad . \tag{4}$$

In addition to a, b, we shall also use the *fatness ratio* $\nu=b/a$ and the *overshooting distance* $\Delta=a-\frac{1}{2}\ell$:

$$v = \frac{b}{a} = \frac{\sqrt{\frac{\lambda}{\ell}}\sqrt{1+\frac{1}{4}\frac{\lambda}{\ell}}}{1+\frac{1}{2}\frac{\lambda}{\ell}} \quad , \qquad \Delta = a - \frac{1}{2}\ell = \frac{1}{4}\lambda \quad . \tag{5}$$

The meaning of fatness ratio v and of overshooting distance Δ is obvious from (5). *Fatness ratio* v is the relative width of the boundary of the Fresnel volume. For high frequencies f, the Fresnel volume is thin, closely concentrated to the ray connecting S and R, with small fatness ratio v. The fatness of the Fresnel volume increases with decreasing frequency (Fig. 1). *Overshooting distance* Δ represents the distance between focus S (or R) and the closest point of the boundary of the Fresnel volume, measured along the rotational axis. It is simple to understand that the overshooting distance does not depend on the distance between the source S and receiver R at all.

We will now consider a high-frequency approximation of (4) and (5), characterised by the relation

$$\lambda \ll \ell \quad . \tag{6}$$

We can neglect the second terms in (4) and (5) containing λ/ℓ and retain only the leading terms:

$$a \approx \frac{1}{2}\ell \quad , \qquad b \approx \frac{1}{2}\sqrt{\lambda\ell} \quad , \qquad v \approx \sqrt{\frac{\lambda}{\ell}} \quad , \qquad \Delta = \frac{1}{4}\lambda \quad . \tag{7}$$

Thus, for $f \to \infty$ quantities b, v and Δ decrease to zero as $b \sim f^{-1/2}$, $v \sim f^{-1/2}$, $\Delta \sim f^{-1}$.

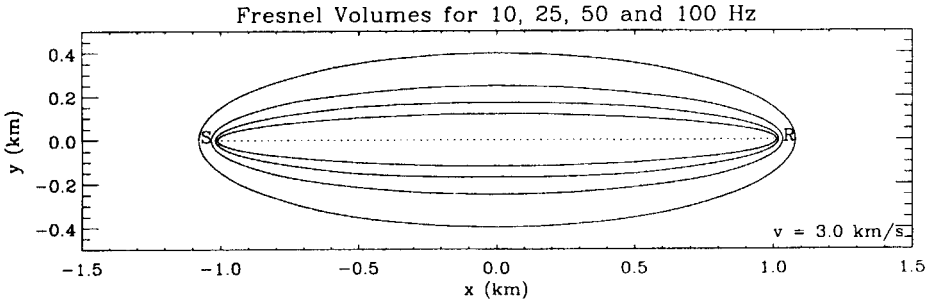

Fig. 1. Boundaries of Fresnel volumes in a homogeneous medium for four frequencies: $f = 10$, 25, 50 and 100 Hz. The distance between source S and receiver R is 1 km and velocity $v = 3$ km/s. The ray connecting S and R is also shown. Note that the boundaries of Fresnel volumes extend beyond source S and receiver R. The relevant distance beyond S (or R) is called the overshooting distance.

2.2 Plane-sectional Fresnel ellipse

We shall now investigate the intersection of Fresnel volume (3) with an arbitrarily oriented plane Σ. It is common knowledge that this intersection of an ellipsoid of revolution with a plane is an ellipse, or a circle. We shall call this intersection the *plane-sectional Fresnel ellipse*. Plane Σ may be arbitrarily inclined with respect to the axis of revolution of the ellipsoid. For planes Σ perpendicular to the rotational axis, we shall speak of the *cross-sectional Fresnel circles*.

First we introduce the following notations: Plane Σ_F as the plane containing the rotational axis of the Fresnel volume and the normal to the plane Σ. If Σ is perpendicular to the rotational axis, Σ_F is an arbitrary plane containing the rotational axis. Without loss of generality, the Cartesian axis x may be oriented along the rotational axis, and the Cartesian axis y in plane Σ_F, perpendicular to the axis x. The Cartesian axis z is then perpendicular to plane Σ_F.

Plane Σ which intersects the Fresnel volume is parallel to the z-axis and intersects the rotational axis at point Q. We shall denote the x-coordinate of Q by x_0, so that $Q = [x_0,0,0]$. We further denote the angle between plane Σ and the y-axis in the xy-plane ψ. Thus, the equation of plane Σ may be expressed as $x = x_0 + y \tan \psi$ (Fig. 2).

The coordinates of points A, B of the intersection of plane Σ with Fresnel volume in plane Σ_F can be obtained by the solution of equations

$$\frac{x^2}{a^2} + \frac{y^2}{b^2} = 1 \quad , \qquad x = x_0 + gy \quad , \tag{8}$$

where $g = \tan \psi$. By solving (8), we obtain the coordinates of A, B,

$$y_{A,B} = \frac{-2x_0 g b^2 \pm \sqrt{D}}{2\left(a^2 + g^2 b^2\right)} \quad , \tag{9}$$

$$x_{A,B} = x_0 + g y_{A,B} = \frac{2x_0 a^2 \pm g\sqrt{D}}{2\left(a^2 + g^2 b^2\right)} \quad , \tag{10}$$

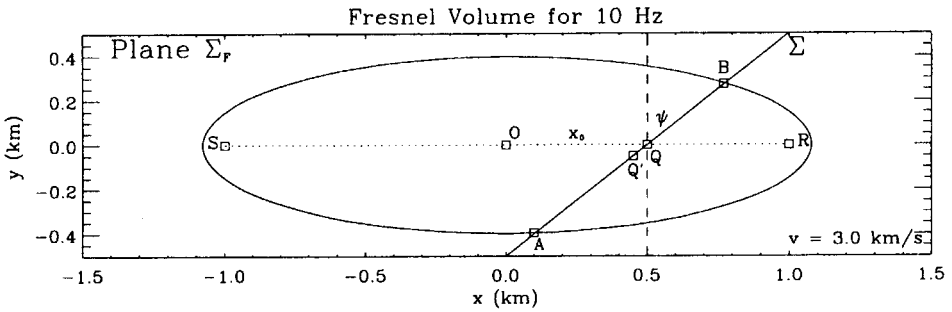

Fig. 2. The intersection of the Fresnel volume with plane Σ. Various notations.

where the discriminant

$$D = 4g^2b^4x_0^2 + 4b^2\left(a^2 - x_0^2\right)\left(a^2 + b^2g^2\right) \quad . \tag{11}$$

We now introduce the in-plane and transverse semi-axes of the plane-sectional Fresnel ellipse, $r^{\parallel}$ and $r^{\perp}$. The *in-plane semi-axis of the plane-sectional Fresnel ellipse* $r^{\parallel}$ is one-half of the distance between A and B:

$$r^{\parallel} = \frac{1}{2}\overline{AB} = \frac{1}{2}\left[\left(x_B - x_A\right)^2 + \left(y_B - y_A\right)^2\right]^{1/2} = \frac{1}{2}\frac{\sqrt{1+g^2}\sqrt{D}}{a^2 + g^2b^2} \quad . \tag{12}$$

The actual center of the plane-sectional Fresnel ellipse is situated at point Q', in the middle between A, B, see Fig. 2. We denote the coordinates of the center Q' of the plane-sectional Fresnel ellipse by $\left[x'_Q, y'_Q, 0\right]$. Hence, in view of (9) and (10),

$$x'_Q = \frac{1}{2}\left(x_A + x_B\right) = \frac{x_0a^2}{a^2 + g^2b^2} \quad , \qquad y'_Q = \frac{1}{2}\left(y_A + y_B\right) = -\frac{x_0gb^2}{a^2 + b^2g^2} \quad . \tag{13}$$

The *transverse semi-axis of the plane-section Fresnel ellipse* $r^{\perp}$ corresponds to the z-coordinate of the boundary of the Fresnel volume at point Q'. Equation (3) then yields

$$r^{\perp} = b\left(1 - \frac{x'^2_Q}{a^2} - \frac{y'^2_Q}{b^2}\right)^{1/2} = b\left(1 - \frac{x_0^2}{a^2 + g^2b^2}\right)^{1/2} \quad . \tag{14}$$

These equations for the in-plane and transverse semi-axis of the plane-sectional Fresnel ellipse may be slightly modified to yield

$$r^{\parallel} = b\frac{\sqrt{1+g^2}}{1+g^2v^2}\sqrt{1 - \frac{x_0^2}{a^2} + g^2v^2} \quad , \tag{15}$$

$$r^{\perp} = \frac{b}{\sqrt{1+g^2v^2}}\sqrt{1 - \frac{x_0^2}{a^2} + g^2v^2} \quad . \tag{16}$$

Here v is the fatness ratio given by (5), and $g = \tan\psi$, $\sqrt{1+g^2} = 1/\cos\psi$.

2.3 The off-ray shift of the center of the plane-sectional Fresnel ellipse

We have obtained an interesting result: The center of the plane-sectional Fresnel ellipse is not necessarily situated on the ray connecting S and R, but may be shifted outside it, to point Q'. We shall call distance $\overline{QQ'}$ the *off-ray shift of the center of the plane-sectional Fresnel ellipse* and denote it d. We can write

$$d = \left[\left(x_Q - x'_Q\right)^2 + \left(y_Q - y'_Q\right)^2\right]^{1/2} = \left[\left(x_Q - x'_Q\right)^2 + y'^2_Q\right]^{1/2} \quad .$$

Using (13), we obtain

$$d = \frac{|x_0 g| v^2}{1 + g^2 v^2} \sqrt{1 + g^2} \quad . \tag{17}$$

Thus, the off-ray shift vanishes in three important cases: a) $x_0 = 0$: Plane Σ passes through the center of Fresnel volume A. b) $g = 0$: Surface Σ is perpendicular to the rotational axis of the Fresnel volume. c) $v = 0$: Frequency f is infinite.

All the relations derived above are exact. They may be used even for a plane-sectional Fresnel ellipse situated completely outside the ray connecting points S and R. This corresponds to $x_0 < -a$ or $x_0 > a$. In this case, it may be suitable to modify Eqs. (15), (16) and (17) slightly.

Instead of $g = \tan \psi$, we introduce $\beta = \operatorname{cotan} \psi = 1/g$. Similarly, instead of x_0 we introduce y_0, the y-coordinate of the intersection of plane Σ with the y-axis. We can then put $x_0 = g y_0$, and Eqs. (15)-(17) yield

$$r^{\parallel} = b \frac{\sqrt{1+\beta^2}}{v^2 + \beta^2} \sqrt{\beta^2 + v^2 - \frac{y_0^2}{a^2}} \quad , \tag{18a}$$

$$r^{\perp} = \frac{b}{\sqrt{v^2 + \beta^2}} \sqrt{\beta^2 + v^2 - \frac{y_0^2}{a^2}} \quad , \tag{18b}$$

$$d = \left|\frac{y_0}{\beta}\right| \frac{v^2}{v^2 + \beta^2} \sqrt{1 + \beta^2} \quad . \tag{18c}$$

We can check the validity of (18) considering the extreme form of the plane-sectional Fresnel ellipse for a plane Σ given by the relation $y = y_0$. This plane Σ is parallel to the ray connecting S and R, and is situated at distance y_0 from it. Using (3), we easily obtain

$$r^{\parallel} = a \sqrt{1 - \frac{y_0^2}{b^2}} \quad , \qquad r^{\perp} = b \sqrt{1 - \frac{y_0^2}{b^2}} \quad . \tag{19}$$

The same result is obtained from (18) if we insert $\beta = 0$ and $v = b/a$. In this case equation (18c) yields the obvious result $d \to \infty$.

2.4 The ratio of in-plane and transverse semi-axes

We shall denote the ratio of in-plane and transverse semi-axes of the plane-sectional Fresnel ellipse ε. Using (15) and (16), we easily obtain

$$\varepsilon = -\frac{r^{\parallel}}{r^{\perp}} = \sqrt{\frac{1+g^2}{1+g^2 v^2}} \quad . \tag{20}$$

For the standard case of the fatness ratio $v < 1$, we have $\varepsilon > 1$. Thus, the in-plane semi-axis $r^{\parallel}$ is, in the standard case, larger than transverse semi-axis $r^{\perp}$,

2.5 The cross-sectional Fresnel zone

If plane Σ is perpendicular to the rotational axis of the Fresnel ellipsoid, angle ψ vanishes and $g = 0$. Then $\varepsilon = r^{\parallel}/r^{\perp} = 1$ and the Fresnel ellipse reduces to the Fresnel circle. We shall call this circle simply the *Fresnel zone* and denote its radius r, $r = r^{\parallel} = r^{\perp}$. The center of the circle is situated directly on the ray, as $d = 0$ for $g = 0$, see (17).

We shall assume that $-a \le x_0 \le a$. Otherwise plane Σ would not intersect the Fresnel volume. Using (15) or (16), we obtain the following equations for the *radius of the Fresnel zone*:

$$r = b\left(1 - \frac{x_0^2}{a^2}\right)^{1/2} \quad . \tag{21}$$

We shall now discuss several special cases of (21). If $x_0 = 0$, point Q is situated at O, and (21) yields $r = b$, as discussed above. If $x_0 = a$, i.e. at the intersection of the x-axis with the boundary of the Fresnel volume, we obtain the expected result $r = 0$. An interesting result is obtained *at the very points S and R*, i.e. for $x_0 = \pm\frac{1}{2}\ell$. Then (21) with (4) yields $r = \frac{1}{2}\lambda$. Thus, the radius of the Fresnel zone directly at sourse S and receiver R is independent of the distance ℓ between S and R, similarly as the overshooting distance. It is, however, twice larger than the overshooting distance.

In the high-frequency approximation (6), equation (21) can be simplified to yield

$$r \approx \frac{1}{2}\sqrt{\lambda\ell}\left(1 - \frac{x_0^2}{a^2}\right)^{1/2} \quad . \tag{22}$$

Here we cannot use (7) for a, but we have to use (4) to obtain the general expression valid in the whole range of x_0, $-a \le x_0 \le a$. Otherwise (22) would fail for x_0 close to $\pm\frac{1}{2}\ell$, i.e.

close to points S and R. Thus, (22) represents an *uniform high-frequency approximation* for r, valid in the whole range of x_0, $-a \le x_0 \le a$. For $|x_0|$ considerably smaller than $\frac{1}{2}\ell$, $|x_0| \ll \frac{1}{2}\ell$, we can insert $a = \frac{1}{2}\ell$ and simplify (21) and (22) even more:

$$r \approx \frac{1}{2}\sqrt{\lambda\ell}\left(1-\frac{4x_0^2}{\ell^2}\right)^{1/2} \tag{23}$$

This equation represents the *local high-frequency approximation*, valid for $|x_0| \ll \frac{1}{2}\ell$ only.

3. FRESNEL VOLUMES AND FRESNEL ZONES OF UNCONVERTED REFLECTED WAVES

We shall now consider a monochromatic unconverted reflected wave at a plane interface Σ between two homogeneous halfspaces. The source is again situated at point S and the receiver at point R. We denote the distance of S from Σ by h_S, and the distance of R from Σ by h_R. We further denote the propagation velocity in the halfspace with S and R by v_1, and the propagation velocity in the second halfspace by v_2. We consider only unconverted reflected waves (*PP,SS*), but not converted reflected waves (*PS,SP*). For converted reflected waves, see *Kvasnička and Červený (1996)*, Section 3.

By reflected waves, we understand the reflected wave in a narrow sense, not contaminated by the structure under the interface. Network ray tracing, however, computes the reflected waves in a broader sense, which corresponds to reflections from the whole medium below interface Σ, see *Kvasnička and Červený (1994)*. Reflected waves in a broader sense also include head waves (if they exist), waves refracted in the second medium and returning into the first medium, etc.

The ray of the reflected wave is fully situated in the plane of incidence which is perpendicular to Σ and passes through S and R. Assume the ray to be incident at point Q of interface Σ. We denote the total length of the ray ℓ, $\ell = \overline{SQ} + \overline{QR}$, the angle of incidence i, with $g = \tan i$, and the horizontal distance between S and R by r.

3.1 The in-plane and transverse semi-axes of interface Fresnel zones

We wish to find the size of the intersection of the Fresnel volume corresponding to an unconverted reflected wave with interface Σ. We shall call it the *interface Fresnel zone*. The simplest way of determining it is to consider an alternative problem, with the image source S' situated symmetrically to S on the other side of interface Σ. For this purpose, we have to consider velocity v_1 also in the second halfspace. The problem to find the Fresnel zone at Σ is then reduced to finding the planar-section of the Fresnel volume (corresponding to S' and R) at interface Σ. See Fig. 3. Let us emphasize that the origin of

the coordinate system is related to point O situated in the middle between S' and R; it is not related to the interface. This problem was treated in Sections 2.2-2.5, so that we can use the equations derived there.

It is not difficult to see that the section of the boundary of the Fresnel volume at interface Σ is an ellipse. One axis of the ellipse is situated in the intersection of Σ with the plane of incidence, and the second is perpendicular to the plane of incidence. We denote the relevant semi-axes of this interface Fresnel ellipse $r^{\parallel}$ and $r^{\perp}$. The *in-plane semi-axis* $r^{\parallel}$ corresponds to the plane of incidence, and the *transverse semi-axis* $r^{\perp}$ to the direction perpendicular to the plane of incidence. The expressions for these two semi-axes correspond to (15) and (16), so that

$$r^{\parallel} = b\frac{\sqrt{1+g^2}}{1+g^2\nu^2}\left(1-\frac{x_0^2}{a^2}+g^2\nu^2\right)^{1/2}, \quad r^{\perp} = b\frac{1}{\sqrt{1+g^2\nu^2}}\left(1-\frac{x_0^2}{a^2}+g^2\nu^2\right)^{1/2} \tag{24}$$

Here we have used the same notation as that used in Section 2.2. Quantities a and b are the semi-axes of the Fresnel volume connecting S' with R and are given by (4), $\lambda = v_1/f$ and ℓ is the distance between S' and R. Quantity again represents the fatness ration, $\nu = b/a$. The angle of incidence i is hidden in g, with $g = \tan i$. Note that $(1 + g^2)^{1/2} = 1/\cos i$. Finally, x_0 measures the distance of point Q, at which the ray is incident at interface Σ, from point O, situated in the middle between S' and R (in the center of the Fresnel volume).

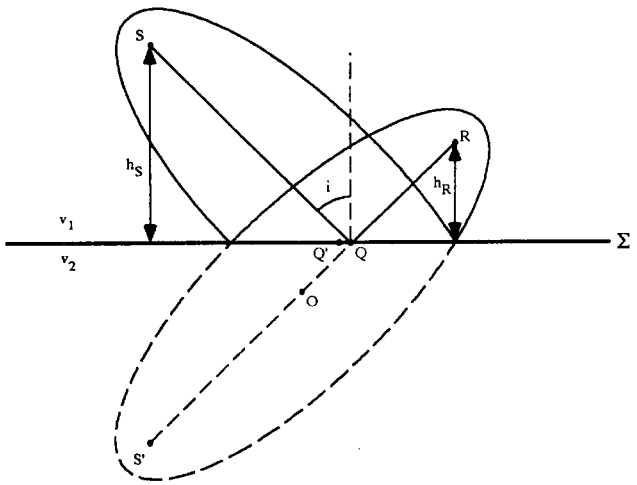

Fig. 3. Computation of the size of the interface Fresnel zone of the unconverted reflected wave at a plane interface. The source and receiver are situated at S and R, the image source at S'. Note that the ray of the reflected wave is incident at the interface at Q, but the center of the interface Fresnel zone is situated at Q'. The distance $\overline{QQ'}$ is called the off-ray shift of the interface Fresnel ellipse.

It will be useful to express ℓ and x_0 in more practical quantities, particularly in terms of h_S, h_R and g. We obtain,

$$x_0 = \frac{1}{2}(h_R - h_S)\sqrt{1+g^2} \quad , \qquad \ell = (h_R + h_S)\sqrt{1+g^2} \quad . \tag{25}$$

Alternatively, we can also use parameters h_S, h_R and r, where r is the horizontal distance between S and R (i.e., the distance between the projections of S and R on Σ). Then r can replace i,

$$g = \tan i = \frac{r}{h_S + h_R} \quad . \tag{26}$$

Let us emphasize one important fact: Equations (24), with (25), (26) and (4), are quite exact for reflected waves in the narrow sense; no approximation was made to derive them.

We shall now consider several special cases of (24):

1. For a zero angle of incidence, $g = 0$, and Eqs. (24) yield,

$$r^{\parallel} = b\left(1 - \frac{x_0^2}{a^2}\right)^{1/2} \quad , \qquad r^{\perp} = b\left(1 - \frac{x_0^2}{a^2}\right)^{1/2} \quad . \tag{27}$$

   Thus, $r^{\parallel} = r^{\perp}$ in this case. Equations (27) are still exact for $i = 0$, but may be used approximately even for small non-zero g. The correction term would be of the order of g^2.

2. For $h_S = h_R$, we have $x_0 = 0$, and we obtain

$$r^{\parallel} = b\left(\frac{1+g^2}{1+g^2v^2}\right)^{1/2} \quad , \qquad r^{\perp} = b \quad . \tag{28}$$

   For $x_0 = 0$, Eqs. (28) are again exact. They may, however, be used approximately even for small $|x_0/a|$. The correction term would be of the order of $|x_0/a|^2$.

3. In the high-frequency approximation, $v \ll 1$. Then

$$r^{\parallel} \approx b\sqrt{1+g^2}\left(1 - \frac{x_0^2}{a^2}\right)^{1/2} \quad , \qquad r^{\perp} \approx b\left(1 - \frac{x_0^2}{a^2}\right)^{1/2} \quad . \tag{29}$$

   These equations represent the *uniform high-frequency approximation*, valid in the whole range of x_0, $-a \le x_0 \le a$, and for high frequencies f. The correction term, with respect to the exact equations (24), would be of the order $(gv)^2 = (b \tan i/a)^2$.

4. The simplest and most useful approximation is the *local high-frequency approximation*, valid for $\lambda \ll \ell$ and $|x_0| \ll \ell$. It is obtained from (29), into which we insert (7) for a and b. The application of (7) for a would considerably decrease its

accuracy, only if x_0 is close to $\frac{1}{2}\ell$, but this would be a very exceptional case. If we use (7) for a and b in (29) we obtain

$$r^{\parallel} \approx \left(\frac{\lambda h_R h_S}{(h_R + h_S)\cos^3 i} \right)^{1/2}, \qquad r^{\perp} \approx \left(\frac{\lambda h_R h_S}{(h_R + h_S)\cos i} \right)^{1/2}. \tag{30}$$

For $h_R = h_S = h$, Eqs. (30) yield,

$$r^{\parallel} \approx \left(\frac{\lambda h}{2\cos^3 i} \right)^{1/2}, \qquad r^{\perp} \approx \left(\frac{\lambda h}{2\cos i} \right)^{1/2}. \tag{31}$$

In (30) and (31) the angle of incidence i can be expressed in term of h_R, h_S and x using (26).

In a general case, the center of the interface Fresnel ellipse is not situated at the point of incidence Q, but is shifted outside the ray, to point Q', see Fig. 3. As in Section 2.3, we shall denote this *off-ray shift* of the center of the interface Fresnel ellipse $d = \overline{QQ'}$. It is again given by expression (17), which is quite general and exact for reflected waves in the narrow sense. As we can see, the off-ray shift vanishes in three cases: a) For $x_0 = 0$, i.e. for the same distance of the source and receiver from Σ. b) For $g = 0$, i.e. for the zero angle of incidence. c) For $v = 0$, i.e. for infinite frequency. If we realize that $v \sim f^{-1/2}$, we can see that $d \sim f^{-1}$. In general, if the interface Fresnel zones are calculated by the paraxial ray method, the off-ray shift obtained is always zero and the center of the paraxial interface Fresnel ellipse is always situated at the point of incidence.

Finally, we shall make a few general remarks concerning the accuracy of the derived equations (24) and (17) with (25), (26) and (4). We again emphasize that these equations are quite exact for reflected waves in the narrow sense (not contamined by the structure below the interface). This particularly applies to the waves reflected from an interface with $v_1 > v_2$. For $v_1 < v_2$, the situation is more complex. In this case the reflected wave in the narrow sense is not well defined in certain regions of angles of incidence. In the critical region, the reflected waves cannot be separated safely from head waves; both these waves form an interference reflected-head wave there (see *Červený and Ravindra*, 1971). To conclude, we can say that for $v_1 < v_2$ the derived equations are not quite exact in the critical region, i.e. for angles of incidence i close to critical angle $i^* = \sin^{-1}(v_1/v_2)$.

3.2 Penetration of the Fresnel volume across interface Σ.

It is obvious that the Fresnel volume of the reflected wave is not limited by interface Σ, but penetrates even across the interface, into the opposite halfspace. See the typical forms of Fresnel volumes of reflected waves in Fig. 5. We denote the maximum depth of the

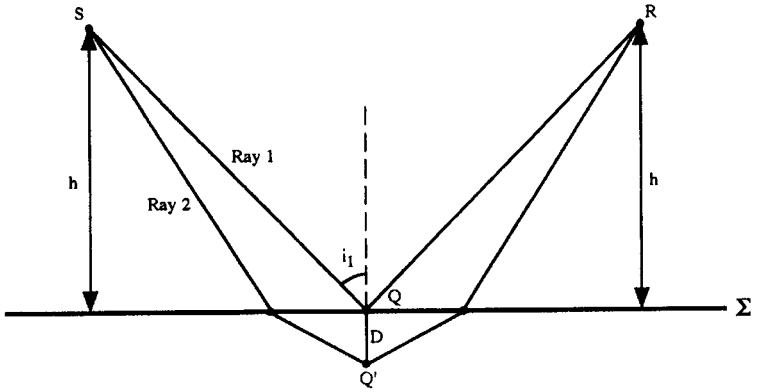

Fig. 4. Schematic diagram for computing the penetration distance D of the Fresnel volume of unconverted reflected waves across interface Σ.

penetration of the Fresnel volume under interface Σ by D and call it the *penetration distance.* Under normal incidence ($g = 0$), the exact expression for D is simple:

$$D = \frac{1}{4}\lambda_2 = \frac{1}{4}v_2 T \quad . \tag{32}$$

Thus, it is exactly the same as the overshooting distance Δ, see (5), only the velocity corresponds to the halfspace below Σ.

For oblique angles of incidence, the exact expression for D would be more complicated. For simplicity, we shall consider only the case $h_S = h_R = h$. It is obvious that the penetration zone is symmetric in this case and that its deepest point Q' is situated in the plane of symmetry between S and R. Penetration distance D then corresponds to the distance of Q' from interface Σ, see Fig. 4.

Mathematically, D can be determined from the equations

$$f_2(p') - f_1(p) = \frac{1}{2}T \quad , \tag{33}$$

$$r = f_3(p) = f_4(p') \quad , \tag{34}$$

where r is the horizontal range between S and R. We have used the notation

$$f_1(p) = rp + 2h\frac{\left(1 - v_1^2 p^2\right)^{1/2}}{v_1} \quad , \tag{35a}$$

$$f_2(p') = rp' + 2h\frac{\left(1-v_1^2 p'^2\right)^{1/2}}{v_1} + 2D\frac{\left(1-v_2^2 p'^2\right)^{1/2}}{v_2} \quad , \tag{35b}$$

$$f_3(p) = 2h\frac{v_1 p}{\left(1-v_1^2 p^2\right)^{1/2}} \quad , \tag{35c}$$

$$f_4(p') = 2h\frac{v_1 p'}{\left(1-v_1^2 p'^2\right)^{1/2}} + 2D\frac{v_2 p'}{\left(1-v_2^2 p'^2\right)^{1/2}} \tag{35d}$$

Here p is the ray parameter along ray 1 ($p = \sin i_1/v_1$), and p' the ray parameter along ray 2. Functions f_1 and f_2 represent travel times, f_3 and f_4 horizontal ranges for the given ray parameters p and p'. Parameters p and p' have to be determined from the known horizontal range r using (34). The system of equations (33) and (34) does not yield simple analytical solutions. It can be solved numerically or approximately.

Before we look for the high-frequency approximate solutions of (33) and (34), we shall derive an alternative form of (33). We insert (35a) and (35b) into (33) and modify it to read

$$\left(r - \frac{2h(p+p')v_1}{\left(1-v_1^2 p^2\right)^{1/2} + \left(1-v_1^2 p'^2\right)^{1/2}}\right)(p'-p) + \frac{2D}{v_2}\left(1-v_2^2 p'^2\right)^{1/2} = \frac{1}{2}T \quad . \tag{36}$$

This equation is still a fully exact alternative of (33). In the paper of *Kvasnička and Červený (1996)*, Eq. (36) will be used to investigate the penetration distance of head waves. Here we shall solve (36) with (34) approximately, for modest angles of incidence and for high frequencies. Then $p' - p$ and D are small. Using equations $r = f_3(p) = f_4(p')$, we can prove that the first term in (36) is of the order of D^2. Neglecting the first term with respect to the second, we finally obtain

$$D \approx \frac{v_2 T}{4\left(1-v_2^2 p^2\right)^{1/2}} \quad . \tag{37}$$

This is the final equation for the penetration distance. It can be expressed in several alternative forms,

$$D \approx \frac{1}{4}v_2 T\left(1-\left(\frac{v_2}{v_1}\right)^2 \sin^2 i\right)^{-1/2} \approx \frac{1}{4}v_2 T\left(1-\left(\frac{v_2}{v_1}\right)^2 \frac{g^2}{1+g^2}\right)^{-1/2} \quad . \tag{38}$$

Equation (38) fails for angles of incidence i close to critical angle i^*, for which $\sin i^* = v_1/v_2$. The square root in (38) is then very small and (38) loses accuracy.

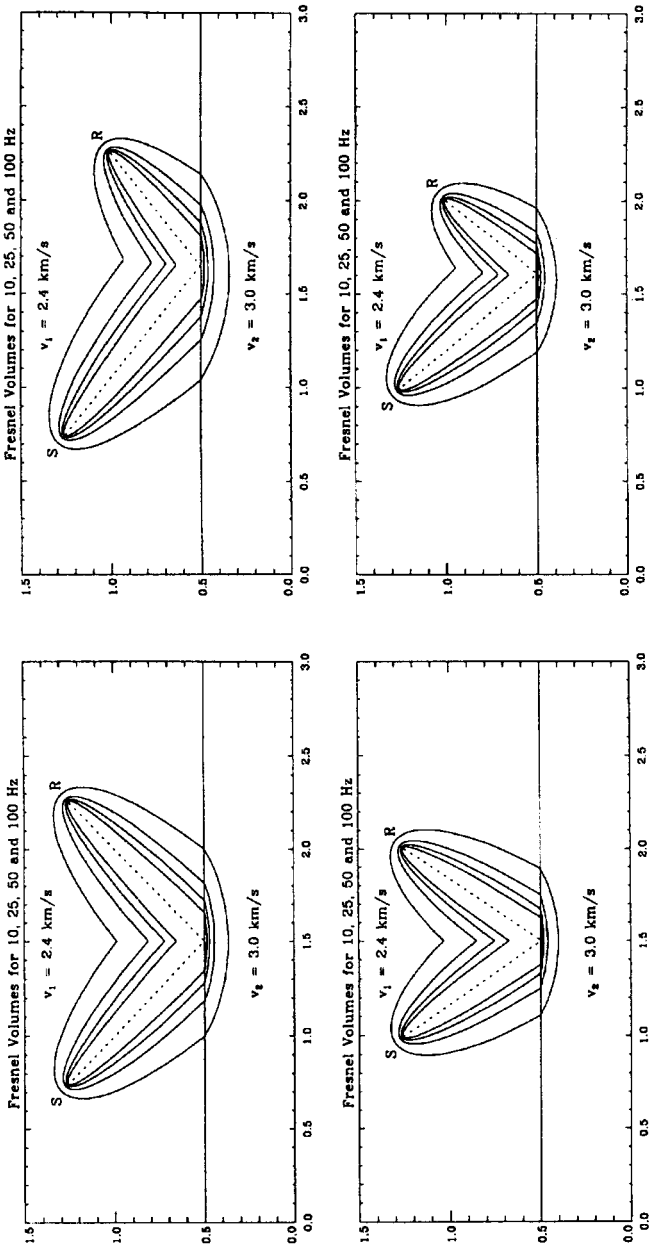

Fig. 5. Boundaries of Fresnel volumes of unconverted reflected waves at plane interface Σ between two homogeneous halfspaces for four frequencies $f = 10$, 25, 50 and 100 Hz. The source is situated at distance $h_S = 0{\cdot}75$ from the interface. The distance h_R of the receiver from the interface is also 0·75 km in the L.H.S. frames and 0·5 km in the R.H.S. frames. The offset is 1·5 km in the upper frame, and 1·0 km in the lower frames. Note the different penetration distances D in the individual frames.

The penetration distance D given by (38) is a useful parameter which tells us how thick a part of the substratum close to the interface is actually affecting the reflected wave field. It also plays an important role in the investigation of the vertical resolution of the seismic method. Thus, using the theory of Fresnel volumes, both the horizontal and vertical resolution can be investigated using a unique approach.

It follows from (32) and (38) that penetration distance D is proportional to f^{-1}. Thus, it cannot be obtained by Fresnel volume ray tracing, based on paraxial ray methods. For $g = 0$, (38) reduces to (32).

3.3 Numerical examples

Fig. 5 shows Fresnel volumes of waves reflected from a plane interface between two homogeneous halfspaces, with velocities $v_1 = 2{\cdot}4$ km/s and $v_2 = 3$ km/s. Four frequencies are considered: $f = 10$, 25, 50 and 100 Hz. In the two frames on the left-hand side, the distances of the source and receiver from the interface are the same, $h_S = h_R = 0{\cdot}75$ *km*. In the other two frames, on the right-hand side, the distance of the source from the interface remains the same, $h_S = 0{\cdot}75$ km, but the distance of the receiver from the interface is smaller, $h_R = 0{\cdot}5$ km. The horizontal ranges between the source and receiver are also different: $r = 1{\cdot}5$ km in the upper two frames, and $r = 1{\cdot}0$ km in the lower two frames. Note that critical distance $r^* = 2$ km for $h_S = h_R = 0{\cdot}75$ km, and $r^* = 1{\cdot}67$ km for $h_S = 0{\cdot}75$ km, $h_R = 0{\cdot}5$ km. The critical angle of incidence is $53{\cdot}13°$, the angle of incidence in the top left-hand frame is 45° and the angle of incidence in the top right-hand frame is $50{\cdot}19°$. Thus, the top right-hand frame represents a receiver situated very close to the critical point; the angle of incidence differs from the critical angle only by $2{\cdot}94°$. All the frames of Fig. 5 have been calculated by network ray tracing, see *Kvasnička and Červený (1994)*. Network ray tracing yields quite accurate results, even in the critical region. It may thus be used as a reference computation to appreciate the accuracy of approximate expressions.

We must, however, remember that network ray tracing yields Fresnel volumes of reflected waves in the broader sense, but the analytical expressions correspond to reflected waves in the narrow sense (not contamined by the head waves in the critical and overcritical regions). We can thus expect some differences between the Fresnel volume computations by different methods, particularly in the critical region.

Let us now discuss the in-plane semi-axis $r^{\parallel}$ of the interface Fresnel ellipse. We shall first compare analytical expressions (24) with the local high-frequency approximation (30). In most cases, both (24) and (30) yield practically the same results. Some differences can be observed only in the critical region. See the top right-hand frame, corresponding to the angle of incidence only $2{\cdot}94°$ less than the critical angle. Even for this extreme case, however, the differences between (24) and (30) do not exceed 6% for $f = 10$ Hz, and are considerably less for higher frequencies. Now we compare $r^{\parallel}$ computed analytically with that obtained by network ray tracing. The comparison again yields quite satisfactory results. The differences between the Fresnel volumes in the broader and narrow sense are again more prominent only in the critical region. In the top right-hand frame, the difference is about 7% for $f = 25$ Hz, and about 4% for $f = 10$ Hz.

Similarly as the relations for $r^{\parallel}$, also the expression for penetration distance D (37) is lower in the critical region. But this was expected. For the critical angle of incidence itself, Eqs. (37)-(38) would yield infinite D. However, the comparison of the analytical computations using (37) and (38) with the frames computed by network ray tracing shows that equations (37)–(38) remain valid for a broad range of angles of incidence, and fail only for angles of incidence very close to the critical angle. The comparisons in three of the frames of Fig. 5 yield a good accuracy. Only in the right-hand upper frame ($h_S = 0{\cdot}75$ km, $h_R = 0{\cdot}5$ km, $r = 1{\cdot}5$ km, $i = 50{\cdot}19°$), the accuracy of the approximate analytic equations is lower. The equations yield $D = 0{\cdot}27$ km, but the correct values measured from Fig. 5 are only about 0·17 km. We have to realize, however, that the angle of incidence is in this case really very close to the critical angle $i^* - i \cong 2{\cdot}94°$. We also have to take into account that equations (37)–(38) have been derived for $h_S = h_R$, but the relevant frame shows D for $h_S \neq h_R$ ($h_S = 0{\cdot}75$ km, $h_R = 0{\cdot}5$ km).

4. CONCLUDING REMARKS

In this paper, we have discussed the Fresnel volumes and Fresnel zones of direct and reflected unconverted waves in simple types of media. This has allowed us to derive simple, but exact expressions for various characteristics of Fresnel volumes and Fresnel zones.

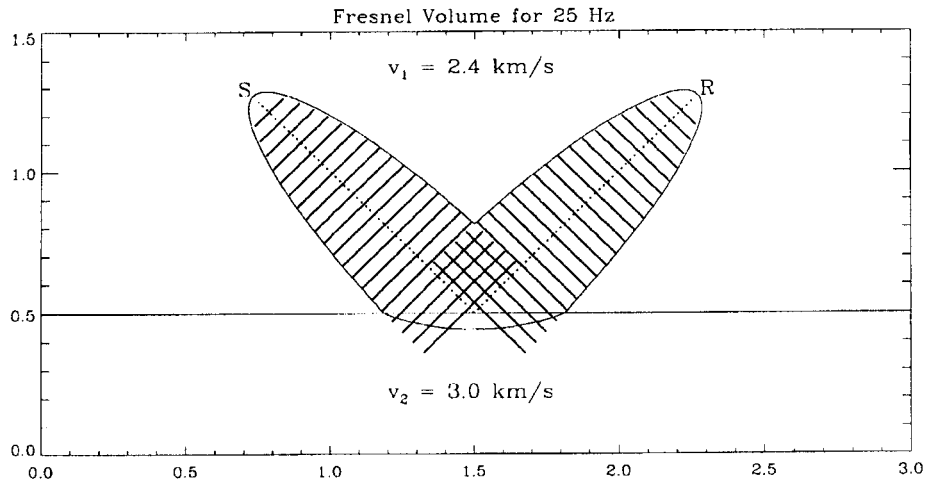

Fig. 6. Comparison of Fresnel volume computations performed by two methods. The same model as in Fig. 5 is considered, with $h_S = h_R = 0{\cdot}75$ km, $f = 25$ Hz. The continuous thin line shows the boundary of the Fresnel volume, computed by network ray tracing similarly as in Fig. 5. The bold lines perpendicular to the ray show the semi-axes r of the Fresnel ellipses computed by Fresnel volume ray tracing. For a detailed discussion see Section 4.

The Fresnel volume ray tracing, based on the paraxial ray method (*Červený and Soares, 1991*) could be applied to the computations of Fresnel volumes and Fresnel zones of various seismic body waves in considerably more complex structures. It *does not*, however, *yield* the correct estimates for certain important parameters which decrease with increasing frequency f as f^{-1}. let us list at least the following four of them:

a) Overshooting distance Δ,
b) The off-ray shift of the center of the plane-sectional Fresnel ellipse,
c) The off-ray shift of the center of the interface Fresnel ellipse,
d) The penetration distance of the Fresnel volume across the interface.

In all these cases, paraxial ray tracing yields zero values.

Fresnel volume ray tracing mostly yields the estimates of certain parameters of the Fresnel volumes and interface Fresnel zones which decrease with increasing frequency as $f^{-1/2}$. These are mainly the following quantities:

a) The semi-axes of the Fresnel volumes,
b) The fatness ratio of the Fresnel volume,
c) The semi-axes of the plane-sectional Fresnel zone,
d) The semi-axes of the interface Fresnel zone.

Even in this case, however, the paraxial ray method yields only an approximate result, not exact. For example, a typical example is the equation for semi-axis b of ellipsoid b. The exact expression is given by (4) and reads $b = \frac{1}{2}\sqrt{\lambda\ell}(1+\lambda/4\ell)^{1/2}$. The paraxial ray approximation for b reads $b \approx \frac{1}{2}\sqrt{\lambda\ell}$, and is of the order of $f^{-1/2}$ for $f \to \infty$. The second term in the square root, which is of the order f^{-1}, is not obtained by the paraxial ray method. Thus, the inaccuracy of the Fresnel volume ray tracing must be taken into account if used for lower frequencies.

To demonstrate the differences between Fresnel volume ray tracing and network ray tracing, Fig. 6 displays the Fresnel volumes computed by both methods. The model is the same as in Fig. 5, with $h_S = h_R = 0{\cdot}75$ km and $r = 1{\cdot}5$ km, see the top left-hand side frame in Fig. 5. The frequency under consideration is 25 Hz. The continuous thin line shows the boundary of the Fresnel volume computed by network ray tracing. The bold lines perpendicular to the central ray show the semi-axes $r^{\parallel}$ of the Fresnel ellipses computed by Fresnel volume ray tracing.

As we can see in Fig. 6, Fresnel volume ray tracing mostly yields sufficiently accurate results with the following three exceptions: a) Fresnel volume ray tracing does not yield the overshooting distances at S and R which equal 24 m in our case, see (5). Close to source S and receiver R, slightly smaller Fresnel zones are obtained by Fresnel volume ray tracing than by network ray tracing. b) Fresnel zones computed by Fresnel volume ray tracing intersect interface Σ close to the point of incidence Q. This is, however, only a formal problem which can be easily solved by a simple modification in the plotting routines. c) Fresnel volume ray tracing does not yield the penetration of the Fresnel volume into the second medium, which is obtained quite safely by network ray tracing.

This is one of the most serious problems in the application of Fresnel volume ray tracing. The maximum penetration distance D in our example computed by network ray tracing is close to 54 m. This is only slightly higher than the 48 m obtained by approximate formula (37). We have to take into account that (37) is valid only for modest angles of incidence.

Note that the interface Fresnel zone is obtained correctly by both methods, and agrees fully with the approximate formula (30) for $r^{\parallel}$. In both cases, $r^{\parallel} \approx 320$ m is obtained. As $h_S = h_R = 0{\cdot}75$ km, the off-ray shift d vanishes.

Acknowledgements: This work was pertially supported by the Elf Geoscience Research Centre, London, U.K., by the Grant Agency of the Charles University under Contracts 8/94 [and 38/94], by the Grant Agency of the Czech Republic under Contract 205/95/1465, and by the European Commission within the framework of the JOULE II Project "Integrated Structural Imaging of Seismic Data".

Manuscript received: 18 January 1995 *Revised: 20 December 1995*

References

Almeida M.A., 1991: Investigação de resolução horisontal no método sísmico utilizando o volume de Fresnel calculado através do traçado do raio. In: *Expanded Abstracts, 2nd International Congress of the Brazilian Geophysical Society*, Salvador, pp. 440–445, Brazilian Geophysical Society, Salvador (in Portuguese).

Ben-Menahem A. and Beydoun W.B., 1985: Range of validity of seismic ray and beam methods in general inhomogeneous media-I. General theory. *Geophys. J. R. astr. Soc.* **82**, 207–234.

Berkhout A.J., 1984: *Seismic resolution.* Geophysical Press, London.

Beydoun W.B. and Ben-Menahem A., 1985: Range of validity of seismic ray and beam methods in general inhomogeneous media- II. A canonical problem. *Geophys. J. R. astr. Soc.* **82**, 235–262

Červený V. and Ravindra R., 1971: *Theory of seismic head waves.* Univ. of Toronto Press, Toronto.

Červený V. and Soares J.E.P., 1992: Fresnel volume ray tracing. *Geophysics* **57**, 902–915.

Gelchinsky B.Ya., 1985: The formulae for the calculation of the Fresnel zones or volumes. *J. Geophys.* **57**, 33–41.

Kleyn A.H., 1983: *Seismic reflection interpretation.* Applied Science Publ. Ltd., New York.

Klimeš L., 1994: Personal communication

Klimeš L. and Kvasnička M., 1994: 3-D network ray tracing. *Geophys. J. Int.* **116**, 726–738.

Knapp R.W., 1991: Fresnel zones in the light of broadband data. *Geophysics* **56**, 354–359.

Kravtsov Yu.A. and Orlov Yu.I., 1979: On the validity conditions of the geometrical optics method. In: *Recent problems of propagation and scattering of waves*, IRE Acad. Sci. USSR, Moscow (in Russian).

Kravtsov Yu.A. and Orlov Yu.I., 1980: *Geometrical optics of inhomogeneous media.* Nauka, Moscow (in Russian).

Kravtsov Yu.A., 1988: Rays and caustics as physical objects. In: E. Wolf (Ed.), *Progress in Optics*, Vol. **26**, 227–348. North-Holland, Amsterdam.

Kravtsov Yu.A. and Orlov Yu.I., 1990: *Geometrical optics of inhomogeneous media.* Springer Series on Wave Phenomena No. 6, Springer-Verlag, Berlin.

Kvasnička M. and Červený V., 1994: Fresnel volumes and Fresnel zones in complex laterally varying structures. *J. Seismic Exploration* **3**, No.3, 215–230.

Kvasnička M. and Červený V., 1996: Analytical expressions for Fresnel volumes and interface Fresnel zones of seismic body waves. Part 2: Tansmitted and converted waves. Head waves. *Studia geophys. et geod.* (in print).

Lindsey J.P., 1989: The Fresnel zone and its interpretative significance. *The Leading Edge* **8**, No.l0, 33–39.

Moser T-J., 1991: Shortest path calculation of seismic rays. *Geophysics* **56**, 59–67.

Moser T-J., 1992: The shortest path method for seismic ray tracing in complicated media. *PhD Thesis*, Inst. of Theoretical Geophysics, Rijksuniversiteit Utrecht.

Sheriff R.E., 1977: Limitations on resolution of seismic reflection and geological details derivable from them. In: C.E. Payton (Ed.), *Seismic stratigraphy - Applications to hydrocarbon explorations. Mem. Am. Assn. Petr. Geol.* **26**, 3–14.

Sheriff R.E., 1980: Nomogram for Fresnel zone calculation. *Geophysics* **45**, 968–972.

Sheriff R.E., 1985: Aspects of seismic resolution. In: O.R. Berg and D.G. Woolverton (Eds.), *Seismic stratigraphy, II. An integrated approach to hydrocarbon exploration. Mem. Am. Assn. Petr. geol.* **39**, 4–27.

Sheriff R.E., 1989: *Geophysical Methods*. Prentice-Hall, Inc.

Sheriff R.E. and Geldart L.P., 1982: *Exploration seismology*, Vol. **I**. Cambridge Univ. Press.

Yomogida K., 1992: Fresnel zone inversion for lateral heterogeneities in the Earth. *PAGEOPH* **138**, 391–406.